Shear viscosity of phase-separating polymer blends with viscous asymmetry

H. S. Jeon[1] and E. K. Hobbie[2]
[1]*Department of Petroleum and Chemical Engineering, New Mexico Institute of Mining and Technology, Socorro, New Mexico 87801*
[2]*National Institute of Standards and Technology, Gaithersburg, Maryland 20899*
(Received 30 January 2001; published 22 May 2001)

Rheo-optical measurements of phase separating polymer mixtures under simple shear flow have been used to investigate the influence of domain morphology on the viscosity of emulsionlike polymer blends, in which the morphology under weak shear is droplets of one coexisting phase dispersed in a matrix of the second. The structure and viscosity of low-molecular-weight polybutadiene and polyisoprene mixtures, phase separated by quenching to a temperature inside the coexistence region of the phase diagram, were measured as a function of shear rate and composition. In the weak shear regime, the data are in qualitative agreement with an effective medium model for non-dilute suspensions of slightly deformed interacting droplets. In the strong shear regime, where a stringlike pattern appears en route to a shear-homogenized state, the data are in qualitative agreement with a simple model that accounts for viscous asymmetry in the components.

DOI: 10.1103/PhysRevE.63.061403 PACS number(s): 83.80.Tc, 83.50.Ax, 47.55.Dz

I. INTRODUCTION

Emulsions, suspensions, and binary fluid mixtures under flows that resemble simple shear are commonly encountered in a variety of industrial processes, from polymer extrusion to the preparation of paints and slurries. Theoretical predictions of the rheological properties of such systems date back to early models for the viscosity of dilute suspensions and emulsions proposed by Einstein [1], Taylor [2], and Oldroyd [3]. More recently, authors such as Choi and Schowalter [4] and Palierne [5] have derived effective-medium theories for the rheological properties of nondilute suspensions of deformable particles. A striking feature of these models is the increasing degree of computational complexity encountered in the nondilute limit, even though the deformation of the droplets is assumed to be infinitesimal. A quantity predicted by such work is the effective shear viscosity of the suspension (η), usually expressed in terms of the viscosity of the suspending medium (η_m), the volume fraction of the suspended droplets (ϕ_d), and the ratio of the viscosities of the two fluids ($\lambda = \eta_d / \eta_m$).

When the mixture is a phase-separating binary fluid in the vicinity of a critical point of unmixing, an additional level of computational complexity emerges due to the coupling between stress and composition that governs the mixing of the two fluids in the presence of the flow field. Onuki [6] has studied the structure and rheology of such systems extensively. In the limit of very weak shear, the flow stabilizes the spinodal instability, leading to a steady-state domain pattern with limited anisotropy, often taking the form of an emulsionlike distribution of moderately deformed, nearly spherical droplets. As the shear rate ($\dot{\gamma}$) increases, the stabilized domains deform and rupture. The mixing effect of the shear field leads to a reduced interfacial tension very close to criticality, where the steady-state domain pattern becomes highly elongated along the direction of flow [7–10], and at sufficiently high shear rates the mixture becomes homogeneous. In most of these studies, the two components are assumed to have equal viscosities. For mixtures whose pure components exhibit viscous asymmetry, the assumption that the viscosities are comparable may have some validity as a leading-order approximation close to the critical point in the regime of strong shear, where the mixture is approaching a homogenized state. In a number of cases of practical interest, however, this may not be the case, and a higher degree of accuracy is desired. Viscous asymmetry, which is often encountered in the common practice of polymer blending, is an important variable, for example, in the stability of cylindrical filaments under shear [11].

In this paper, we use light scattering, optical microscopy, and rheometry to study the relationship between domain morphology and shear viscosity in low-molecular-weight blends of polybutadiene and polyisoprene undergoing phase separation in the presence of simple shear flow. In the weak shear regime, where the droplets are only slightly deformed, the viscosity data are in qualitative agreement (without any free parameters) with the Choi-Schowalter effective medium model for nondilute suspensions of deformable, interacting droplets [4]. In the strong shear regime, where stringlike patterns appear en route to shear-induced homogenization, the interfacial contribution to the viscosity of a symmetric binary mixture ($\lambda = 1$) should vanish, since the unit vector normal to the domain interface is everywhere perpendicular to the flow field [8]. Here, we find that the shear viscosity exhibits a discontinuity at the phase-inversion point, and we make a simple physical argument that relates this behavior to the viscosity ratio.

II. MATERIALS AND METHODS

A. Materials

The polymers used in this study were synthesized at Goodyear Tire and Rubber Company [12]. The number-averaged relative molecular mass (M_n), the mass-averaged relative molecular mass (M_w), and the polydispersity were determined by gel permeation chromatography, and the microstructure was probed using ^{13}C nuclear magnetic resonance. The polymer chains are statistical copolymers composed of 1-4, 1-2 isomers and 1-4, 3-4 isomers, respectively. The polybutadiene (PB) has a mole fraction of 1-2 isomers

 ©2001 The American Physical Society

equal to 0.1, while the polyisoprene (PI) has a mole fraction of 3-4 isomers equal to 0.07. In general, $M_n = 51\,000$ and $M_w/M_n = 1.04$ for the PB, while $M_n = 88\,000$ and $M_w/M_n = 1.08$ for the PI. The blends were prepared via solution blending from methylene chloride (mass fraction polymer 0.02) containing the appropriate amount of each component and a small amount (mass fraction 0.0005) of Goodyear Wingstay #29 antioxidant. The mixture was stirred at room temperature for 1 day and filtered through a 0.45 μm Gelman Acrodisc CR PTFE filter. The solvent was then evaporated under an atmosphere of flowing nitrogen gas, and the sample was dried in a vacuum oven at room temperature for several days. All shear experiments were performed at 130 °C, where the blends are immiscible under quiescent conditions. The samples were heated from room temperature to 130 °C and held for 120 min before shearing to obtain a reproducible initial two-phase morphology for each sample.

B. Instrumentation

The *in situ* light scattering and optical microscopy instrument, capable of collecting two-dimensional light scattering data and real-time microscopy images in the flow/vorticity plane, was designed and constructed for conducting optical measurements of complex fluids under simple shear flow [13]. The sample compartment is composed of two electrically heated quartz plates, and the temperature of each plate is controlled to within ± 0.5 K by a 100 Ω platinum-resistance-temperature-detector element in conjunction with a 1 mA current source. The gap between the plates was fixed at 465 μm. A beam of vertically polarized monochromatic light from a 15 mW He-Ne laser (wavelength $\lambda = 632.8$ nm) was directed through the sample. The image of the scattered light in the angular range 4–27°, corresponding to wave vector (q) values ranging from 0.23 to 1.54 μm^{-1}, was focused onto a thermoelectrically cooled two-dimensional charge-coupled-device (CCD) detector using a pair of spherical condensers, and the array of data from the 256×256 pixel CCD camera was then transferred to a personal computer. The microscope image is collected with a different CCD camera (Dage MTI, model 72), recorded onto a super-VHS tape, and digitized using a frame grabber from Data Translation (DT 3851). A Rheometrics Scientific SR-5000 rheometer in parallel-plate geometry was used for steady shear measurements of the viscosity, which were carried out with 25 mm diameter fixtures and 0.4 ± 0.01 mm gap thickness. The temperature was controlled to within ± 0.5 K, and the measurements were carried out under a nitrogen atmosphere to prevent any thermal degradation of the polymers, which are known to be sensitive to heat.

C. Phase diagram

The phase-separation temperature of the blend was determined by phase-contrast optical microscopy. Conventional bright field microscopy relies on a significant refractive index difference between the two phases in order to resolve the image. In the case of phase-separated PB/PI blends, it is difficult to obtain a well-resolved image with bright-field microscopy because the refractive index difference between the two components is small ($n_{PB} = 1.512$ and $n_{PI} = 1.517$) [14]. An advantage of this small optical contrast, however, is that multiple scattering effects are suppressed when light scattering is used to probe the morphology. The coexistence curve was determined using a step heating method [15]. The sample was heated in 5-K increments and then allowed to anneal for 120 min. Near the transition temperature, the intervals were reduced to 2 K for greater accuracy. Phase separation was apparent as the formation of droplets, or domain structures, during the 120-min intervals, while samples in the single-phase region appear as featureless, blank images. The PB/PI blend has a lower critical solution temperature of (61.5 ± 0.5) °C at $\phi_c = 0.43$.

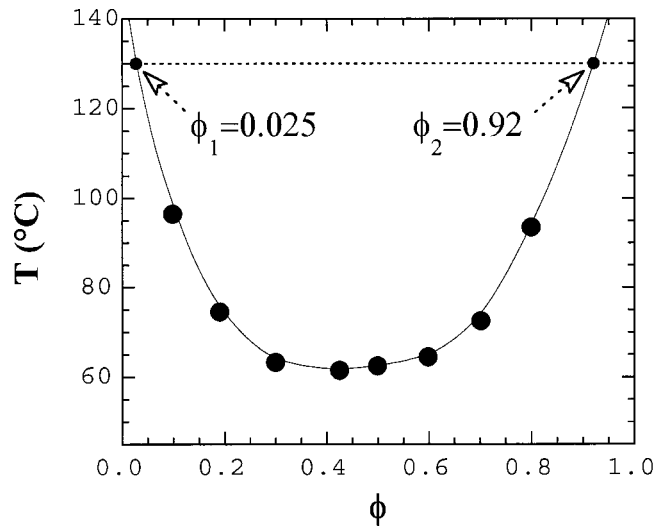

FIG. 1. Phase diagram of the PB/PI system in the temperature/PI-volume-fraction (T-ϕ) plane, where the large markers are data points and the curve is an empirical fit of the data. The horizontal dashed line shows the fixed quench depth of 130 °C, and the two small markers indicate the extrapolated PI volume fractions of the two coexisting phases.

III. RESULTS AND DISCUSSIONS

The measured phase diagram in the temperature PI-volume-fraction (T-ϕ) plane is shown in Fig. 1. From a spline fit of this data, we extrapolate the PI volume fractions of the two coexisting phases after a quench to 130 °C; $\phi_1 = 0.025$ and $\phi_2 = 0.92$. For an arbitrary PI volume fraction ϕ, the volume fractions of the two coexisting phases are given by the lever rule [16]: $x_1 = (\phi_2 - \phi)/(\phi_2 - \phi_1)$ and $x_2 = (\phi - \phi_1)/(\phi_2 - \phi_1)$. A previous study [17] suggests that this system phase inverts at $\phi = 0.55$, implying that for $\phi < 0.55$ the volume fraction of droplets is $\phi_d = x_2$, while for $\phi > 0.55$ the volume fraction of droplets is $\phi_d = x_1$. In the following analysis, we assume that these volume fractions do not change with shear rate, which is probably not rigorously correct [7]. The highest shear rate considered here is 10 s^{-1}, where the morphology is stringlike on both sides of the phase inversion point. Although some mixing has undoubtedly occurred at this point [7,9], these blends typically do not become completely homogenized until shear rates of about 100 s^{-1}, and thus this assumption serves as a useful first

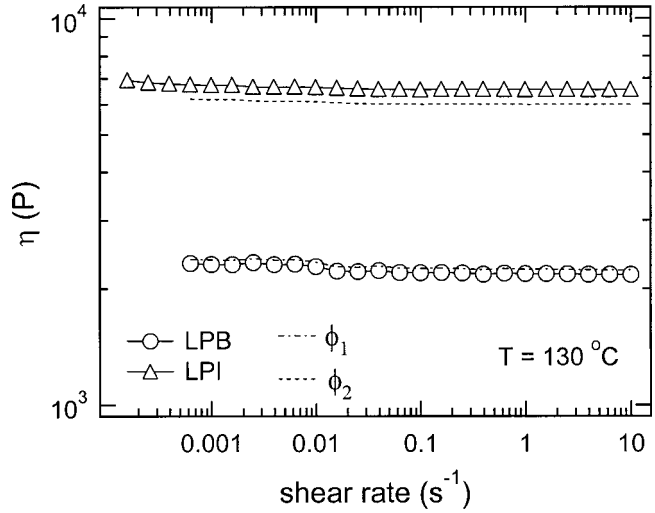

FIG. 2. Steady shear viscosity of the pure melt components as a function of shear rate at 130 °C. The two dashed lines are the viscosities of the two coexisting phases assuming a log-additive mixing rule.

approximation. In Fig. 2 we show the shear viscosity of both of the pure melt components at 130 °C. No evidence of significant shear thinning is evident in either component up to the highest shear rate considered in this study. Knowing the pure melt viscosities, the viscosities of the two coexisting phases at 130 °C can be calculated from ϕ_1 and ϕ_2 assuming a log-additive mixing rule [18], and these values are indicated as dashed lines in Fig. 2. For $\phi<0.55$, the viscosity ratio is thus $\lambda=2.67$, while for $\phi>0.55$, the viscosity ratio is $\lambda=0.37$.

Figure 3 shows light-scattering/micrograph pairs at different shear rates for $\phi=0.40$ at 130 °C, where the width of each micrograph is 200 μm and the scattering patterns subtend an angle of 27° [for the corresponding wave-vector range, see Sec. II B]. The flow direction is to the right and the gradient direction is into the page. At this composition, which is close to critical, the morphology has coarsened into well-defined PI-rich droplets in a PB-rich matrix before the shear is applied. At $\dot{\gamma}=0.001\,s^{-1}$, the coarsening of the domains is stabilized by the shear flow, and the steady-state morphology is emulsionlike, with a polydisperse distribution of essentially spherical droplets [Fig. 3(a)]. At $\dot{\gamma}=0.01\,s^{-1}$, the flow starts to deform the droplets so that the projection into the flow-vorticity plane becomes extended along the flow direction [Fig. 3(b)]. At $\dot{\gamma}=0.1\,s^{-1}$, the droplets have started to burst and the anisotropy has become more pronounced. A stringlike pattern with an extremely high aspect ratio in both real and reciprocal spaces has emerged at $\dot{\gamma}=10\,s^{-1}$ [Fig. 3(d)].

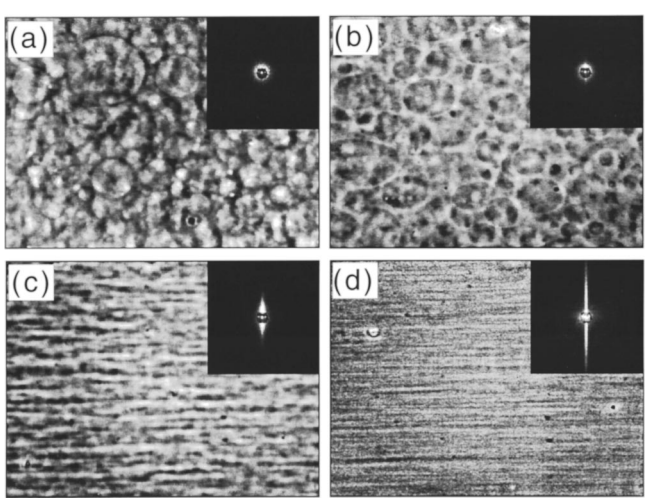

FIG. 3. Light-scattering/micrograph pairs at different shear rates for $\phi=0.40$, where the width of each micrograph is 200 μm and the scattering pattern subtends an angle of 27°. The droplets are PI-rich in a PB-rich matrix, at (a) 0.001, (b) 0.01, (c) 0.1, and (d) 10 s^{-1}. The flow direction is to the right and the gradient direction is into the page.

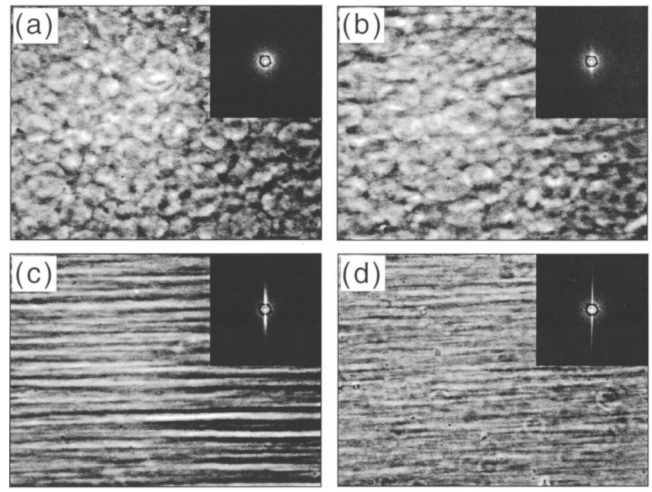

FIG. 4. Light-scattering/micrograph pairs at different shear rates for $\phi=0.60$, where the width of each micrograph is 200 μm and the scattering pattern subtends an angle of 27°. The droplets are PB-rich in a PI-rich matrix, at (a) 0.001, (b) 0.01, (c) 0.1, and (d) 10 s^{-1}. The flow direction is to the right and the gradient direction is into the page.

Figure 4 shows light-scattering/micrograph pairs at different shear rates for $\phi=0.60$ at 130 °C, where again the width of each micrograph is 200 μm and the scattering patterns subtend an angle of 27°. Here, the droplets are PB-rich in a PI-rich matrix. The overall evolution of the anisotropy is qualitatively quite similar to that exhibited at $\phi=0.40$ (Fig. 3); however, the steady-state morphology at higher shear rates [Figs. 4(c) and 4(d)] is coarser, which can be most easily seen by comparing Figs. 3(c) and 4(c). The origin of this difference probably lies in the viscous asymmetry of the two components. For isolated droplets, filamentlike structures generally do not occur in shear flow for $\lambda>1$, while for $\lambda<1$ they do [19]. Thus, the domains in Fig. 4 are readily extended to high aspect ratios at shear rates where those in shown Fig. 3 tend to rupture. The appearance of a stringlike pattern at high shear rates when the viscosity ratio is greater than or comparable to unity has been previously attributed to a shear-induced decrease in the interfacial tension due to the homogenizing effect of the shear flow [7]. Shear-induced coalescence, however, likely plays an equally important role,

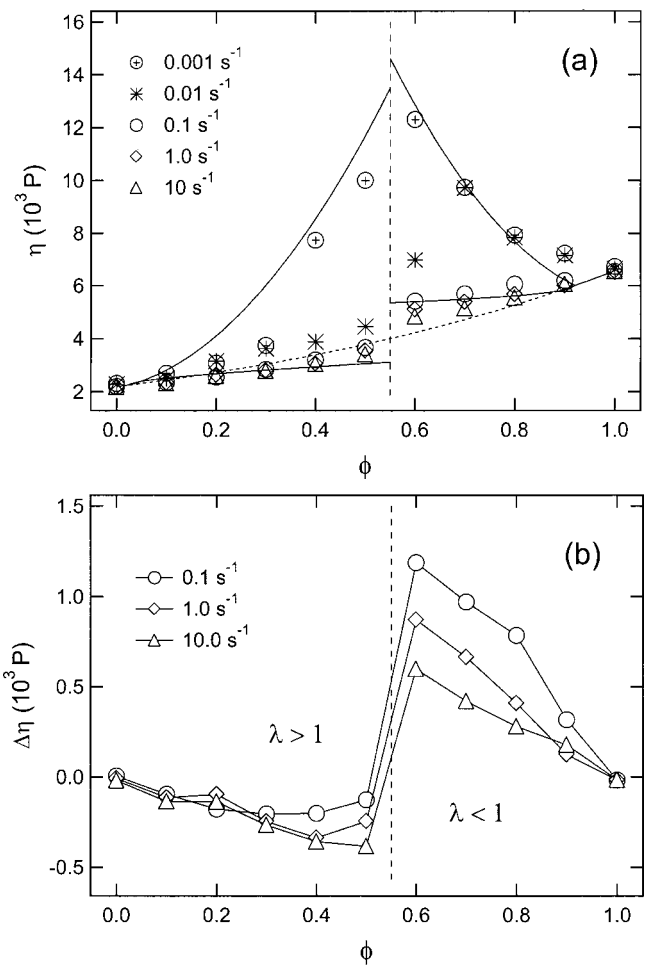

FIG. 5. (a) Shear viscosity of the blends for different shear rates as a function of the PI volume fraction, where the dashed curve is the viscosity of the homogenized mixture, assuming log-additivity of the melt viscosities. The upper curve is the theoretical prediction for slightly deformed droplets from Ref. [4], and the lower curve is a fit based on the simple physical model derived in the text. At $\phi = 0.55$ (vertical dashed line) the system phase inverts from PI-rich droplets to PB-rich droplets, and the shear viscosity exhibits a discontinuity. (b) Excess shear viscosity as a function of PI volume fraction in the strong shear regime, where $\lambda > 1$ for $\phi < 0.55$ and $\lambda < 1$ for $\phi > 0.55$.

particularly in mixtures with significantly different melt viscosities for which $\lambda > 1$.

Figure 5(a) shows the steady-state shear viscosity of the blend at four different shear rates as a function of the PI volume fraction at 130 °C, where the dashed curve is the viscosity of the homogenized mixture calculated assuming log-additivity of the melt viscosities [18]. The vertical dashed line in Fig. 5 indicates the phase inversion point, where ϕ_d switches from x_2 to x_1, λ inverts to $1/\lambda$, and the shear viscosity exhibits a discontinuity [17]. The upper, solid curve is the theoretical prediction for a nondilute suspension of deformable particles derived by Choi and Schowalter [4].

$$\eta \approx 1 + \phi_d \frac{(5\lambda+2)}{2(\lambda+1)} + \phi_d^2 \frac{5(5\lambda+2)^2}{8(\lambda+1)^2} + \cdots . \tag{1}$$

There are no free parameters in this comparison with theory, which gives a reasonable description of the data for $\dot{\gamma} = 0.001\,\mathrm{s}^{-1}$. Two exceptions are $\phi = 0.20$ and 0.30, where the theory appears to overestimate the blend viscosity significantly. At $\dot{\gamma} = 0.01\ \mathrm{s}^{-1}$, where the droplets are substantially deformed and ellipsoidal in shape, the above analysis (which is derived for nearly spherical droplets) would appear to be inadequate.

At the three highest shear rates, the domain morphology is stringlike and the blend viscosity is relatively insensitive to shear rate. The data suggest a slight reduction in viscosity (relative to the homogenized state) in the regime where $\lambda > 1$, and a slight enhancement in the regime where $\lambda < 1$, with a discontinuity at the phase inversion point. This behavior can be seen more clearly by plotting the calculated excess viscosity, $\Delta\eta = \eta - \eta_0$, as a function of PI composition [Fig. 5(b)], where η_0 is the calculated viscosity of the homogenized mixture [dashed curve, Fig. 5(a)]. A simple but physical explanation for this behavior might lie in the details of the blend morphology, which depends strongly on shear rate. In general, the volume fraction of strings is

$$\phi_d \sim \pi D^2/\ell^2, \tag{2}$$

where D is the mean string diameter and ℓ is the mean separation between strings in the gradient-vorticity plane. Consider a volume element of height h along the gradient direction. If the lower surface of this volume element is at rest, then the top surface will move at a rate

$$\nu \sim N_s D \dot{\gamma}_d + (h - N_s D)\dot{\gamma}_m , \tag{3}$$

implying an effective shear rate ν/h, where $\dot{\gamma}_d$ is the shear rate in a string, $\dot{\gamma}_m$ is the shear rate in the matrix, and $N_s \sim h/\ell$ is the mean number of strings in the flow-gradient plane. Note that continuity of tangential shear stress across an interface implies $\eta_d \dot{\gamma}_d \sim \eta_m \dot{\gamma}_m$. The effective viscosity is thus

$$\eta_{\mathrm{eff}} \approx \eta_m \dot{\gamma}_m h/\nu \approx \eta_m \left\{ 1 + \left(\frac{\phi_d}{\pi}\right)^{1/2} \left(\frac{1}{\lambda} - 1\right) \right\}^{-1} . \tag{4}$$

In the limit $\phi_d \to 0$, Eq. (4) reduces to the viscosity of the matrix, as it should. The opposite limit ($\phi_d \to 1$) is inappropriate, as the system inverts. A fit of the data to this expression is shown as the lower solid curve in Fig. 5(a). To generate this comparison with theory, the matrix viscosity was fixed asymptotically and λ was varied as a free parameter, giving $\lambda = 2.8$ for $\phi < 0.55$ and $\lambda = 0.75$ for $\phi > 0.55$. These values can be compared with the accepted values of 2.67 and 0.37, respectively. Although it might be argued that the model is physical, since it gives order-of-magnitude agreement with experiment, a more detailed and quantitative theoretical treatment is clearly needed.

IV. CONCLUSIONS

Based on Fig. 5, the viscosity of the phase-separated blend would appear to be quite sensitive to the specific

steady-state domain morphology, which varies from emulsionlike distributions of nearly spherical domains under weak shear to highly asymmetric stringlike filaments under moderate to strong shear. Although of great practical and fundamental significance, critical blends with viscous asymmetry have received little or no computational attention. For moderately deformed domains, models of the type proposed in Ref. [4] would appear to have some validity when applied to blends, which amounts to treating the stabilized phase-separating mixture as a nondilute suspension of deformable particles. For modest to extreme deformations, one can in principle find similar analogies with existing rheological models of highly deformed emulsions, similar to but more sophisticated than the simple physical model proposed in the previous section. One essential feature that such models would ignore, however, is the critical-dynamic aspect of the problem that dominates when the mixture is in the vicinity of a consolute point. Calculations of the type described in Ref. [6] and simulations of the type described in Ref. [10] that incorporate viscous asymmetry would be particularly useful and relevant, and it is hoped that the work described here will help guide and motivate such a formalism.

ACKNOWLEDGMENTS

The authors are grateful to C. C. Han, A. I. Nakatani, and A. Chakrabarti for useful and enlightening discussions during the course of this work, as well as to Goodyear Tire and Rubber Company for the synthesis and contribution of the polymer samples used in this study.

[1] A. Einstein, Ann. Phys. (Leipzig) **19**, 289 (1906); **34**, 591 (1911).
[2] G. I. Taylor, Proc. R. Soc. London, Ser. A **138**, 41 (1932).
[3] J. G. Oldroyd, Proc. R. Soc. London, Ser. A **218**, 122 (1953).
[4] S. J. Choi and W. R. Schowalter, Phys. Fluids **18**, 420 (1975).
[5] J. F. Palierne, Rheol. Acta **29**, 204 (1990).
[6] A. Onuki, Phys. Rev. A **35**, 5149 (1987).
[7] E. K. Hobbie, S. Kim, and C. C. Han, Phys. Rev. E **54**, R5909 (1996); J. W. Yu, J. F. Douglas, E. K. Hobbie, S. Kim, and C. C. Han, Phys. Rev. Lett. **78**, 2664 (1997).
[8] T. Hashimoto, K. Matsuzaka, E. Moses, and A. Onuki, Phys. Rev. Lett. **74**, 126 (1995).
[9] L. Kielhorn, R. H. Colby, and C. C. Han, Macromolecules **33**, 2486 (2000).
[10] Z. Shou and A. Chakrabarti, Phys. Rev. E **61**, R2200 (2000).
[11] A. Frischknecht, Phys. Rev. E **56**, 6970 (1997); **58**, 3495 (1998).
[12] Materials, instruments, and services are specified in this paper to give a detailed account of the work, and do not imply an endorsement by NIST or the Federal Government.
[13] S. Kim, J.-W. Yu, and C. C. Han, Rev. Sci. Instrum. **67**, 3940 (1996).
[14] J. Brandrup and E. H. Immergut, *Polymer Handbook*, 3rd ed. (Wiley-Interscience, New York, 1989), Chap. IV, p. 455.
[15] L. Sung, D. B. Hess, C. L. Jackson, and C. C. Han, J. Polym. Res. **3**, 139 (1996).
[16] P. M. Chaikin and T. C. Lubensky, *Principles of Condensed Matter Physics* (Cambridge University Press, Cambridge, England, 1995), p. 484.
[17] H. S. Jeon, A. I. Nakatani, E. K. Hobbie, and C. C. Han, Langmuir (to be published); H. S. Jeon, A. I. Nakatani, C. C. Han, and R. H. Colby, Macromolecules **33**, 9732 (2000).
[18] Qualitatively, if a quantity (like viscosity) exhibits an Arrhenius (or barrier-activated) temperature dependence, then the argument of the exponential, which takes the form of an enthalpy, is an extensive quantity that should scale with volume fraction. Hence for a miscible mixture of two fluids A and B, the effective viscosity should be well approximated by $\ln(\eta) = \phi_A \ln(\eta_A) + \phi_B \ln(\eta_B)$. This widely used relation is known as the ''log-additive mixing rule.'' See, for example, S. Glasstone, K. L. Laidler, and H. Eyring, *Theory of Rate Processes* (McGraw-Hill, New York, 1941).
[19] G. I. Taylor, Proc. R. Soc. London, Ser. A **146**, 501 (1934).